Title

CD3+CD56+ and CD3−CD56+ lymphocytes in the cerebrospinal fluid of persons with HIV-1 subtypes B and C

Authors

de Almeida, Sergio M
Beltrame, Miriam Perlingeiro
Tang, Bin
et al.

Publication Date

2023-04-01

DOI

10.1016/j.jneuroim.2023.578067

Peer reviewed

HHS Public Access

Author manuscript

J Neuroimmunol. Author manuscript; available in PMC 2024 January 26.

Published in final edited form as:

J Neuroimmunol. 2023 April 15; 377: 578067. doi:10.1016/j.jneuroim.2023.578067.

$CD3^{+}CD56^{+}$ and $CD3^{-}$ $CD56^{+}$ lymphocytes in the cerebrospinal fluid of persons with HIV-1 subtypes B and C

Sergio M. de Almeida[a,*], **Miriam Perlingeiro Beltrame**[b], **Bin Tang**[c], **Indianara Rotta**[a], **Julie Lilian P. Justus**[b], **Yara Schluga**[b], **Maria Tadeu da Rocha**[b], **Edna Martins**[b], **Antony Liao**[c], **Ian Abramson**[c], **Florin Vaida**[c], **Rachel Schrier**[c], **Ronald J. Ellis**[c]

[a]Virology Laboratory, Hospital de Clínicas, Universidade Federal do Paraná, Curitiba, PR, Brazil

[b]Immunophenotyping Laboratory, Hospital de Clínicas, Universidade Federal do Paraná, Curitiba, PR, Brazil

[c]HIV Neurobehavioral Research Center (HNRC), UCSD, San Diego, CA, USA

Abstract

The transactivator of transcription (Tat) is a HIV regulatory protein which promotes viral replication and chemotaxis. HIV-1 shows extensive genetic diversity, *HIV-1 subtype C* being the *most* dominant *subtype* in the world. Our hypothesis is the frequency of CSF $CD3^{+}CD56^{+}$ and $CD3^{-}$ $CD56^{dim}$ is reduced in HIV-1C compared to HIV-1B due to the Tat C30S31 substitution in HIV-1C. 34 CSF and paired blood samples (PWH, $n = 20$; PWoH, $n = 14$) were studied. In PWH, the percentage of $CD3^{+}CD56^{+}$ was higher in CSF than in blood ($p < 0.001$) comparable in both compartments in PWoH ($p = 0.20$). The proportion of $CD3^{-}$ $CD56^{dim}$ in CSF in PWH was higher than PWoH ($p = 0.008$). There was no subtype differences. These results showed CNS compartmentalization of NKT cell response in PWH.

Keywords

Human immunodeficiency virus (HIV); HIV-1C; Natural killer (NK) cells; T lymphocytes with natural killer activity; (NKT); Flow cytometry; Immunophenotyping

1. Introduction

Natural killer (NK) lymphocytes play a significant role in the control and prevention of HIV-1 infections. HIV infection disrupts the phenotypes and functions of monocytes, NK cells, and innate lymphoid cells, and subsequently, the relevant adaptive host immune responses (Alter and Altfeld, 2009; Tomescu et al., 2011).

[*]Corresponding author at: Complexo Hospital de Clínicas–UFPR, Seção de Virologia, Setor Análises Clínicas, Rua Padre Camargo, 280, Curitiba, PR 80060-240, Brazil. sergio.ma@ufpr.br (S.M. de Almeida).

Declaration of Competing Interest

The authors have no conflicts of interest to declare regarding the publication of this article.

Appendix A. Supplementary data

Supplementary data to this article can be found online at https://doi.org/10.1016/j.jneuroim.2023.578067.

T lymphocytes with natural killer activity (NKT cells) are $CD3^+$ T cells that co-express CD56, CD16, CD57, and CD69 (Uemura et al., 2008; Zhou et al., 2013; Bojarska-Junak et al., 2010). NKT cells are part of the innate immune system and play an important role in the immune response to viruses (Lanier et al., 1986; Elewaut and Kronenberg, 2000). They are usually derived from lymphokine (mainly interleukin-2)-activated T-cells (Tarazona et al., 2000; Olteanu et al., 2010). Antigens typically associated with NK cells may also be expressed on T cells, particularly $CD8^+$ T cells that have a large granular lymphocyte cytology and cytotoxic function similar to that of NK cells (Tarazona et al., 2000). Although NKT cells constitute a small proportion of lymphocytes in normal individuals, this subset of T cells may be expanded in the presence of chronic immune system activation, as can be seen in autoimmune disorders or viral infections. They also provide support and help to B cells which act as a microbial defense (Tarazona et al., 2000; Olteanu et al., 2010).

NK cells constitute approximately 10% of the mononuclear cells in human peripheral blood (PB), and their function is regulated by a number of germline-encoded activating/inhibitory receptors that orchestrate their activation (Raulet, 2003). The predominance in the cerebrospinal fluid (CSF) of the adaptive immune system CD4 T cells over those of the innate immune system may be related to the fact that under normal circumstances, the CNS is much less exposed to pathogens (and auto-antigens) than peripheral organs (de Graaf et al., 2011). It has been suggested that NK cells play a key role at the interface of innate and adaptive responses in autoimmune diseases (Moretta et al., 2008; Nguyen et al., 2002). NK cells contribute to both the effector and regulatory functions of innate immunity via their cytotoxic activity and ability to secrete pro- and anti-inflammatory cytokines and growth factors [Mayo et al., 2012]. NK cells have been classified into two major subsets based on their surface expression of CD56 (neural cell adhesion molecule, NCAM). $CD3^-$ $CD56^{bright}$ NK cells represent approximately 10% of PB NK cells, whereas $CD3^-$ $CD56^{dim}$ NK cells represent approximately 90% (Cooper et al., 2001; Michel et al., 2016; Taborda et al., 2014). The differences between these two subsets also include their homing molecules and effector capacities. $CD3^-$ $CD56^{dim}$ cells are considered mature NK cells; these cells originate from a differentiation process involving the loss of inhibitory receptors (Moretta, 2010). $CD3^-$ $CD56^{dim}$ are effector NK cells, which are predominant in PB, have reduced proliferative capacity, and produce negligible amounts of cytokines, but are highly cytotoxic (Caligiuri, 2008). In contrast, the more immature (naive) subset, $CD3^-$ $CD56^{bright}$, is regulatory, found in secondary lymphoid tissue and from other tissues, and is able to proliferate and secrete a large range of cytokines, although they have minimal cytotoxic capacity (Poli et al., 2009). Naïve $CD3^-$ $CD56^{bright}$ cells dominate CSF (Gross et al., 2020). Overall, NK cells are expected to boost the immune response within the CNS (Huang et al., 2006; Bielekova et al., 2006). Paradoxically, NK cells appear to have an inhibitory role in autoimmune responses within the CNS.

Tat protein plays a pivotal role in the induction of chemokine secretion, mainly by CC chemokines (β-chemokines) (Kutsch et al., 2000). *Tat* also upregulates the expression of several cytokines including TNF-α (Chen et al., 1997; Bennasser and Bahraoui, 2002), which is attributed to the C30C31 dicysteine motif (Albini et al., 1998; Beall et al., 1996). In vitro studies have suggested that HIV-1 subtype C (HIV-1C) is less neuropathogenic than subtype B based on a defective *Tat* chemokine dimotif in the C30S31 position that might

influence cellular trafficking and CNS inflammation (Ranga et al., 2004; Williams et al., 2020). In a Brazilian population, the frequency of the C30S31 substitution in HIV-1 Tat C was 82% vs. 10% in HIV-1B ($p < 0.0001$; de Almeida et al., 2021). However, we did not find that subtype C Tat was associated with less neurocognitive impairment than subtype B (de Almeida et al., 2013).

It was demonstarted that HIV-1 Tat inhibits NK cell function by blocking L-type calcium channels (Zocchi et al., 1998), the same group found that the Tat C- terminal domain inhibited NK cell activation by dendritic cells (Poggi et al., 2002).

Since NK cell subset imbalance has been observed in subjects chronically infected with HIV (Hu et al., 1995; Mavilio et al., 2003; Alter et al., 2005; Milush et al., 2013; Björkström et al., 2010), we measured the frequencies of the two major NK cell subsets ($CD3^-$ $CD56^{bright}$ and $CD3^-$ $CD56^{dim}$) in all HIV-infected subjects to verify that the NK cell subset distribution in our subject cohort confirmed previous findings (Hu et al., 1995; Mavilio et al., 2003; Alter et al., 2005; Milush et al., 2013; Björkström et al., 2010).

The present study aimed to 1) assess the relative frequencies of NKT ($CD3^+CD56^+$) and NK ($CD3^-$ $CD56^{dim}$ or $CD3^-$ $CD56^{bright}$) cells in the CSF and PB, 2) determine whether they differ in people with HIV (PWH) and without HIV (PWoH, HIV-negative controls) and between people with HIV-1 subtypes B and C, 3) perform secondary exploratory comparisons to evaluate the relationship between NKT and NK cell subpopulations and HIV RNA in CSF and PB, and 4) explore differences in proportions of lymphocytes between groups categorized by the distribution of HIV RNA in both compartments. We hypothesized that the relative frequency of NKT cells and NK subsets in the CSF would be HIV-1 subtype-dependent such that people with HIV-1C would have a lower proportion of NKT and NK cells than those with HIV-1B due to the Tat C30S31 cysteine substitution in HIV-1 subtype C.

2. Methods

2.1. Ethics statement

This study was conducted in accordance with the principles of the Declaration of Helsinki. The protocols were approved by the institutional review board of the Hospital de Clínicas, Universidade Federal do Paraná (HC-UFPR, Curitiba, Paraná, Brazil). Written informed consent was obtained from all participants prior to their enrollment in the study.

2.2. Study design and participants

This cross-sectional study explored monocyte phenotypes in the CSF of a subset of participants enrolled in the HC-UFPR study. In this study, 36 PB and 34 paired CSF samples were collected from 36 participants recruited from Curitiba, Southern Brazil (PWH, $n = 22$; PWoH, $n = 14$). HIV-1 subtypes were genotyped using the *pol* or *env* sequences. Genotyping revealed that eight individuals were infected with HIV-1B, while 14 were infected with non-B HIV-1 subtypes (C, $n = 9$; BF, $n = 3$; CF, n = 1; and F, n = 1). In 9 participants the subtype HIV-1B or C was confirmed by the Tat sequencing (de Almeida et al., 2021). All

HIV-1B sequences ($N = 4$) showed Tat sequence C30C31, and all HIV-1C ($N = 5$) showed C30S31.

In the PWoH group, 14 age-matched subjects who underwent surgery under spinal anesthesia were recruited. The indications for surgery were hernia (n = 3), lower limb varicose veins (n = 3), column surgery (n = 2), hysterectomy (n = 2), knee surgery (n = 2), hemorrhoidectomy (n = 1), and perineoplasty (n = 1). These participants had no neurological comorbidities or cognitive complaints, and had negative serological tests for HIV, hepatitis C virus, and syphilis. The CSF inclusion criteria for this group were as follows: white blood cell (WBC) count ≤5 cells/mm^3, total protein ≤45 mg/dL, and glucose ≥55 mg/dL.

All volunteers underwent serological testing to confirm their HIV status before enrollment (Brasil, 2018). The PWH recruited did not have opportunistic CNS infections.

Demographic data, clinical and HIV infection characteristics, comorbidities, and biochemical, cytological, and virological characteristics of the CSF samples are shown in Table 1.

2.3. CSF and peripheral blood samples

The relative frequency of each lymphocyte population was determined using paired CSF and PB samples from both the groups. CSF samples were collected via lumbar puncture (LP) without the addition of an anticoagulant, and PB samples were collected with the addition of ethylenediaminetetraacetic acid (K3 EDTA 7.5%).

2.4. Laboratory methods

2.4.1. Immunophenotyping—Multiparameter flow cytometry was used to identify and quantify cellular phenotypes in CSF and PB. Immunophenotyping was performed on fresh CSF samples processed within 20 min of LP. Preservative medium was not added.

PB samples were collected at the time of LP and processed in parallel with the CSF. Fresh CSF samples (4–6mL) were centrifuged at 500 ×*g* at room temperature for 5min. The supernatant was aspirated, and not decanted to prevent excessive cell loss, and the cell pellets were resuspended in 300 μL of 0.5% bovine serum albumin (BSA) and gently mixed. The goal was to obtain at least 5000 events per tube. The cells were mixed well by inversion and WBCs were counted using a hemocytometer (Sysmex, Roche, USA).

2.4.2. Sample processing—For the conventional technique, fresh PB samples containing 10^6 cells and 100 μL of blood were incubated for 15 min at room temperature in the dark with pre-titrated saturating amounts of four-color combinations of fluorochrome-conjugated and *monoclonal antibody* (MoAb). An additional unstained sample was processed in parallel to serve as a negative control. Non-nucleated red blood cells were lysed using FACS lysing solution (BD Biosciences, San Jose, CA, USA) according to the manufacturer's instructions. The remaining cells were sequentially centrifuged at 500 ×*g* at room temperature for 5min, washed twice in phosphate-buffered saline PBS (pH 7.4) or PBS plus 0.5% BSA (pH 7.4), and resuspended in 300 μL of PBS for FC acquisition and analysis

(Craig et al., 2011). For each PB sample aliquot, a minimum of 50,000 events were acquired using the CellQUEST software (BD Biosciences).

2.4.3. Flow cytometry analysis—CSF and PB cells were analyzed for surface markers expression using flow cytometry. The cells were stained for flow cytometry with the following monoclonal antibodies: control mouse isotypes and anti-human CD45 conjugated with peridinin chlorophyllprotein/cyanin 5 (PerCP-Cy5.5), anti-human CD3 conjugated with fluorescein isothiocyanate (FITC; BD Biosciences, San Jose, CA, USA), and anti-human CD56 conjugated with phycoerythrin (PE, Beckman Coulter, CA, USA).

The cells were labeled with optimal concentrations of these monoclonal antibodies. CSF cell staining was performed at room temperature in the dark, and washes and incubations were performed in 0.5% PBS/BSA. Whole PB samples were labeled for 15 min at room temperature and then lysed with 2mL lysis solution (Becton Dickinson, San Jose, CA, USA). The cells were then washed twice. For data acquisition and analysis, a flow cytometer (FACSCalibur ™ Four Color, BD Biosciences, San Jose, CA, USA) with Infinicyt software 2.0 (Cytognos, Salamanca, Spain) was used. $CD3^{+}CD56^{+}$ (NKT) and $CD3^{-}$ $CD56^{+}$ (NK) lymphocytes were analyzed within the CD45 + -gated region. NK cell subsets $CD56^{dim}$ and $CD3^{-}$ $CD56^{bright}$ were identified according to the staining intensity with the specific mAb.

The characterization of circulating NKT cell subsets was performed without CD16 and with the CD56 marker ($CD3^{+}CD56^{+}$), as described previously (Krijgsman et al., 2019; El-Hagrasy and Hassanein, 2019; Rodríguez-Martín et al., 2015).

The $CD3^{-}$ $CD56^{dim}$/ $CD3^{-}$ $CD56^{bright}$ ratio was calculated to analyze the effector/regulatory function.

The entire cell suspension was acquired for CSF samples. The median (interquartile range; IQR) of events acquired and analyzed, for the total cell populations was 242 (132; 615) events, the percentage of cell visibility was 29.40% (17.25%; 50.60%). The events acquired and analyzed for $CD3^{+}CD56^{+}$ (NKT) were 226 (132; 576) and for $CD3^{-}$ $CD56^{+}$ were 0.0 (0.0; 20) events. CSF samples with fewer than 10 cells (events) acquired in the phenotype gate were considered to have zero events (Quijano et al., 2009). The percentage of positive cells was measured from a cut-off set using an isotype-matched nonspecific control antibody. The gating strategy used for flow cytometry experiments to define $CD3^{+}CD56^{+}$ and $CD3^{-}$ $CD56^{+}$ subpopulations were developed for PB samples and applied to CSF samples (Supplementary Figs. 1 and 2).

2.4.4. Clinical laboratory measurements—Nadir $CD3^{+}CD4^{+}$ counts were retrieved from the medical records. Total CSF protein, glucose, and white blood cell (WBC) counts were quantified using standard laboratory methods. The total CSF WBC count (cells/mm^3) was quantified using fresh, non-centrifuged CSF samples immediately after LP.

2.4.5. Quantification of plasma and CSF HIV RNA levels—HIV RNA levels in PB and CSF were quantified using the *m*24*sp and m2000* Real-Time System (Abbott, Chicago, IL, USA) with 1 mL of CSF or plasma. The assays were performed immediately

after sample collection. Samples with HIV RNA levels of >40 copies/mL were within the detection limit. The data are presented as $\log_{10}$ values. HIV groups were categorized based on the quantification of HIV RNA in paired CSF and PB samples. When CSF > PB, the discordance between levels was defined as the CSF HIV RNA level with any value greater than the PB viral load, PB > CSF, and suppressed (aviremic) in both compartments.

2.5. Data analyses

The demographic and HIV disease characteristics and CSF biochemical, cytological, and virology measures are presented as the median (IQR or range) or number (%), as appropriate, and compared in individuals infected with HIV-1B and –1C using the independent samples *t*-test for continuous variables and Fisher's exact test for binary and categorical variables. Similar methods were used for comparisons between PWH (including subtypes B, C, BF, BC, CF, and F) and PWoH.

The proportion was assigned a missing value if the denominator (event) was zero.

Comparisons of monocyte subsets in CSF versus PB, PWH vs. PWoH, and HIV-1B vs. HIV-1C in CSF and PB were performed separately using linear regression. To stabilize the variance and improve normality properties, the proportion of monocyte subsets was arcsine square root-transformed prior to statistical analysis.

For some lymphocyte subsets, the Wilcoxon test was used due to highly skewed data; Welch's two-sample t-test was conducted when two groups had unequal variance (i.e., variance =0 for one group). Multiple testing correction for multiple related biomarkers was performed using the Benjamini-Hochberg (BH) procedure or Tukey's honestly significant difference (HSD) test, as appropriate. Age and sex were considered as covariates in the biomarker comparisons between the PWH and PWoH groups, and blood/CSF HIV viral load suppression as covariates in the biomarker comparisons between HIV-1B and –1C.

In the exploratory analysis, PWH were categorized into three groups (i.e., CSF > PB, CSF < PB, and aviremic) based on the distribution of HIV RNA in the CSF and PB. The proportions of NKT and NK lymphocytes in the CSF and PB were compared among the groups using the Kruskal-Wallis test, and pairwise comparisons were performed using the Mann-Whitney test.

Correlation coefficients (ρ) were estimated using Spearman's rank-order method; for example, the correlations between the proportions of NKT and NK lymphocytes in CSF and PB, the main lymphocyte and monocyte subpopulations in CSF and PB (described in detail in de Almeida et al., 2022), CSF characteristics (WBC count and total protein), CSF and PB HIV RNA, nadir $CD3^+CD4^+$, PB $CD3^+CD4^+$ recovery, duration of infection, and CNS antiretroviral Penetration-Effectiveness Rank (CPE, Letendre et al., 2010), were estimated using Spearman's rank-order method.

R (version 3.4.1) was used to perform statistical analyses. The significance level of α was set at 5%. The effect size (ES), analogous to Cohen's d (and 95% confidence interval [Cis]), was estimated as the coefficient divided by the residual standard deviation.

3. Results

3.1. Subject characteristics

Subject demographics, HIV disease status, and CSF characteristics are presented in Table 1. The age and sex were comparable between the PWH and PWoH groups. Among PWH, the median (IQR) CD4 nadir was 219 (33, 532) cell/mm^3; median plasma HIV RNA (log_{10}) was 1.60 (1.60, 3.21); 68% were on ART, and 14 (63.64) were suppressed.

Individuals infected with HIV-1C and HIV-1B did not differ in age and HIV infection characteristics, including duration of infection, CSF and plasma HIV RNA, nadir CD4 counts, CSF WBC count, and frequency of cases on ART ($p > 0.05$), but differed in sex (33.3% females vs. 100% males, $p = 0.009$).

3.2. $CD3^+CD56^+$ lymphocytes (NKT cells) in CSF and PB

The proportion of $CD3^+CD56^+$ lymphocytes in PWH was lower than that in PWoH (2.00% vs. 7.10%, $p < 0.001$) in PB, but comparable in CSF (7.95% vs. 5.05, $p = 0.210$). PWH had a higher proportion of $CD3^+CD56^+$ lymphocytes in the CSF than in the PB (Cohen's d = 1.03, 95% CI = 0.50–1.56, p < 0.001), but were comparable in both compartments in the PWoH group ($p = 0.200$) (Table 2; Fig. 1a).

In the comparisons between HIV-1 subtypes B and C, the proportion of $CD3^+CD56^+$ lymphocytes was comparable in the CSF and PB. In the HIV-1B group, the proportion of $CD3^+CD56^+$ lymphocytes in the CSF was higher than that in PB [d = 1.33, 95% CI = 0.35–2.31, $p = 0.016$; $p = 0.011$ in the model controlling for plasma HIV RNA). In the HIV-1C group, CSF with PB had comparable proportions of NKT cells (Table 3; Fig. 1a).

The frequency of CSF samples with detectable $CD3^+CD56^+$ lymphocytes was comparable between the PWH and PWoH groups [15/18 (83.33%) vs. 10/14 (71.43%), respectively, $p = 0.669$], as well as between HIV-1B and HIV-1C CSF samples [6/7 (85.71%) vs. 4/6 (66.67%), respectively, $p = 0.559$].

3.3. NK lymphocytes subsets in CSF and PB

In PWH in CSF and PB predominated $CD3^-$ $CD56^{dim}$; in PB, the medians of $CD3^-$ $CD56^{dim}$ and $CD3^-$ $CD56^{bright}$ were greater than those in PWoH; CSF $CD3^-$ $CD56^{dim}$ levels were undetectable in PWoH.

The proportion of $CD3^-$ $CD56^{dim}$ lymphocytes in the CSF of PWH was higher than that in PWoH (d = 0.99, 95% CI = 0.31–1.68, $p = 0.008$). Concerning HIV-1 subtypes B and C, the proportion of $CD56^{dim}$ lymphocytes was comparable in the CSF and PB (Table 3; Fig. 1b). In the PB samples, the proportion of $CD3^-$ $CD56^{dim}$ lymphocytes was higher in the PWoH group than in the PWH group ($p = 0.030$ and $p = 0.060$, respectively).

$CD3^-$ $CD56^{dim}$ and $CD3^-$ $CD56^{bright}$ lymphocytes were not identified in any CSF sample from PWoH, while $CD3^-$ $CD56^{bright}$ lymphocytes were identified in one CSF sample from PWH (Table 2, Fig. 1b).

The relative frequency of CSF samples with detectable $CD3^-$ $CD56^{dim}$ lymphocytes was higher in PWH than in PWoH (8/20 vs. 0/14, p = 0.011) and numerically higher in patients with HIV-1C than in those with HIV-1B; however, the difference was not significant (5/8 vs. 2/7, $p = 0.315$).

In the comparison between HIV+ and HIV−, p value was adjusted for age and gender in the adjusted model, and then corrected for multiple testing with the BH method within CSF and blood and cell subtype separately; all p-values were corrected for multiple testing using the BH method; [(b)] p-values before and after the BH correction. Group differences are presented as Cohen's d; CI, confidence interval; the Cohen's d (95%CI) effect sizes for the comparisons between blood and CSF (A vs. C and B vs. D) are shown in Supplementary Table 1; [(c)] effector / regulatory ratio.

3.4. $CD3^+CD56^+$ and $CD3^-$ $CD56^+$ lymphocyte subpopulations in the CSF and peripheral blood of PWH categorized according to HIV RNA in both compartments

Based on HIV RNA in the CSF and PB compartments, PWH were categorized into three groups: CSF > PB and CSF < PB in viral load (people with unsuppressed VL) and aviremic in CSF and PB (people with suppressed VL). The proportions of $CD3^+CD56^+$ and $CD3^-$ $CD56^{dim}$ lymphocytes in the CSF and PB were comparable among the three groups (Table 4, Fig. 1c and d).

The frequency of CSF samples with detectable $CD3^+CD56^+$ lymphocytes was numerically higher in the aviremic group (10/11, 91.00%) than in the CSF > PB group (2/3, 66.67%) and PB > CSF group (3/4, 75%), but the difference was not statistically significant ($p = 0.534$). In contrast, the frequency of CSF samples with detectable $CD3^-$ $CD56^{dim}$ lymphocytes was higher in the viremic group (CSF > PB, 2/3, 66.67%; PB > CSF, 3/4, 75%) than in the aviremic group (3/13, 23.07%), although this difference was also not statistically significant ($p = 0.106$). The frequency of $CD3^-$ $CD56^{dim}$ in the CSF was significantly higher in the groups with unsuppressed viral load in both CSF and PB than in the PWoH group (Fig. 1e, $p = 0.022$ and 0.005 for the comparisons of a vs. d and b vs. d, respectively). Comparisons between the unsuppressed groups (a and b) and the aviremic group (c) were not statistically significant ($p > 0.05$). Additionally, the frequency of $CD3^+CD56^+$ in the CSF was higher in the aviremic group than in the unsuppressed group, but the difference was not statistically significant (p > 0.05).

The frequency of CSF samples with $CD3^-$ $CD56^{dim}$ was significantly higher in PWH with unsuppressed viral loads in both CSF and PB than in the PWoH group (Fig. 1e, p = 0.022 and 0.005 for the comparisons of a vs. d and b vs. d, respectively). Comparisons between the unsuppressed groups (a and b) and the aviremic group (c) were not significant (p > 0.05). Additional, the frequency of CSF samples with $CD3^+CD56^+$ was higher in the aviremic group than the unsuppressed group but the p-value in comparison was not significant (p > 0.05).

The PB $CD3^-$ $CD56^{dim}$/ $CD3^-$ $CD56^{brigt}$ ratio was numerically reduced in the aviremic group compared with the PWoH group, although not significantly (Supplementary Fig. 4).

3.5. Correlations

In the PWH group, increases in the proportion of CSF $CD3^{-}$ $CD56^{dim}$ lymphocytes correlated with decreases in CSF and PB $CD3^{+}$ lymphocytes [$\rho = -0.684$, $p = 0.0009$ and $\rho = -0.500$, $p = 0.025$, respectively]. In this group, higher proportions of CSF $CD3^{-}$ $CD56^{dim}$ lymphocytes correlated with higher HIV RNA in CSF and PB ($\rho = 0.651$, $p = 0.002$ and 0.433, $p = 0.056$, respectively) and with higher proportions of $CD14^{++}CD16^{+}$ in CSF ($\rho = 0.554$, $p = 0.021$) (Fig. 2a, b, f), but with lower proportions of CSF and PB $CD3^{+}$ lymphocytes and PB $CD14^{++}CD16^{+}$ ($\rho = -0.684$, p = 0.0009; −0.500, p = 0.025 and −0.639, $p = 0.004$, respectively) (Fig. 2d, e, g). The proportions of CSF and PB $CD3^{-}$ $CD56^{dim}$ lymphocytes were also strongly correlated ($\rho = 0.749$, $p = 0.0001$) (Fig. 2c). In addition, we found that there was an increase in the proportion of CSF $CD3^{-}$ $CD56^{dim}$ cells when the CSF WBC count increased ($\rho = 0.507$, $p = 0.023$).

There was no correlation between CSF $CD3^{+}CD56^{+}$ lymphocytes and any of the variables of interest, including PB $CD3^{+}CD56^{+}$ ($\rho = 0.016$, $p = 0.950$), as well as CSF or PB HIV RNA ($\rho = -0.114$, $p = 0.652$ and $\rho = -0.209$, $p = 0.404$ respectively). However, PB $CD3^{+}CD56^{+}$ lymphocytes were positively correlated with PB $CD3^{-}$ $CD56^{dim}$ and $CD3^{-}$ $CD56^{bright}$ ($\rho =$ 0.457 and 0.505, respectively).

The relationship between PB $CD3^{-}$ $CD56^{dim}$ lymphocytes and CSF variables of interest is shown in Supplementary Fig. 3.

4. Discussion

In the present study, we analyzed the proportion of NKT and NK cells in the CSF and PB between PWH and PWoH and assessed the differences in the proportions of these cells between HIV-1B and HIV-1C subtypes.

While the fact that NKT cells are expanded in chronic infection is already known (Slauenwhite and Johnston, 2015), the finding of NKT cells were significantly high in the CSF, but not PB, of PWH compared to healthy controls is a meaningful observation. These results showed compartmentalization of the innate immune response cell levels in PWH, with levels in the CSF being higher than levels in the blood, but comparable between HIV-1B and HIV-1C. These differences were not driven by CSF HIV RNA as there was no correlation between CSF or PB HIV RNA and CSF $CD3^{+}CD56^{+}$ lymphocytes.

Persistent CNS inflammation and chronic immune activation play important roles in neuronal damage in HIV-associated neurocognitive disorders (HAND) (de Almeida et al., 2016; Zipeto et al., 2018; Ruhanya et al., 2021). In response to both peripheral and intrathecal inflammation, CD3 + CD56+ cells may be more likely to travel to the CNS, than in its absence, or these cells may be retained or survive for longer in the CSF compartment. Inflammatory factors driving differential accumulation of these cells to the CSF are associated with tissue expression of chemokines, which provide insights into how NKT cells establish tissue tropisms (Kim et al., 2002). NKT cells are specialized in both cytokine production and expression of chemokine receptors (Kim et al., 2002). The impact of infection on the tissue localization and function of NKT remains largely understudied

(Slauenwhite and Johnston, 2015). The trafficking machinery of NKT, including expression of chemokine receptors, is not clear. Most NKT cells express CCR1, CCR2, CCR5, CXCR3, CXCR4, and CXCR6, these chemokine ligands (MIP-1α, MCP-1, MIP-1β, IP-10) are widely expressed in extra-lymphoid tissues and up-regulated by inflammatory signals (Kim et al., 2002). These chemokines are associated with HAND pathophysiology (de Almeida et al., 2016). Studies about CNS NKT cells transmigration are even more limited. MCP-1 and its receptor CCR2 are primarily expressed by microglia (Monteiro de Almeida et al., 2005; Conductier et al., 2010).

The percentage of NKT cells in PB in PWH was lower than that in PWoH; however, for CSF, PWH and PWoH did not differ. The reduced PB NKT cell population in PWH individuals is likely due to a combination of factors, which include direct HIV-1 infection of NKT cells and subsequent cell death, impaired generation and/or responsiveness to cytokines that promote NKT cell survival, and tissue redistribution of NKT cells (Slauenwhite and Johnston, 2015). The fact that, in our study, NKT cells are significantly higher in the CSF than PB, could represent the redistribution of NKT cells to the CNS.

NKT cells are highly susceptible to infection with HIV-1 due to the expression of multiple co-receptors for viral fusion and entry, including CD4 and the chemokine receptors CCR5, CXCR4, and CXCR6 (Kim et al., 2002; Motsinger et al., 2002; Fleuridor et al., 2003). The results of this study point to the contribution of NKT cells to the CNS influx of HIV. The lack of correlation of CSF NKT cells with CSF or PB HIV RNA do not corroborate this hypothesis. However, the limited number of samples limits any robust conclusion.

The role of NKT cells in HIV-1 infection remains unclear since some studies report no correlation between NKT cell numbers and HIV disease progression, while others have suggested an association between higher levels of CD4+ NKT cells and lower plasma viremia (Motsinger et al., 2002; Slauenwhite and Johnston, 2015). In our study, there was no correlation of NKT cells in CSF or PB with any of the variables of interest, including the HIV infection characteristics (i.e. CSF and PB HIV RNA, nadir $CD3^+CD4^+$, PB $CD3^+CD4^+$ recovery, duration of infection, and CPE).

In this study, there was a higher number of samples with NK cells identified in the PWH group than in the PWoH group, which is in accordance with the described function of these cells. The proportion of CSF $CD3^-$ $CD56^{dim}$, which are effector cells, increased with greater immunological impairment (lower PB $CD3^+$) and higher CSF and PB HIV RNA. NK cells are functionally defined by their ability to spontaneously lyse virally infected or tumor cells without major histocompatibility complex (MHC) restriction. A small proportion of the $CD3^-$ $CD56^+$ NK cell subset has been described in normal individuals, representing <2% of PB lymphocytes (Trinchieri, 1989).

Similar to our study, the distribution of $CD3^+CD56^+$ cells in the CSF and PB of healthy volunteers without history of any neurological or other major medical disorders was comparable (Svenningsson et al., 1995). In individuals without neurological diseases, the percentage of CSF NKT and NK cells is <5% in most CSF samples (de Graaf et al., 2011; Svenningsson et al., 1993, 1995; Kowarik et al., 2014).

In this study, CSF analysis revealed that the majority of CSF NK cells were $CD3^{-}$ $CD56^{dim}$ cells in the PWH group, which contrasts what has been found in individuals with multiple sclerosis (MS) or other diseases associated with neuroinflammation, where the majority of intrathecal NK cells were $CD3^{-}$ $CD56^{bright}$ (Gross et al., 2016; Hamann et al., 2013). Enhanced adhesion and transmigration of this subset across primary human brain microvascular endothelial cells (HBMECs) suggest that the increased proportion of $CD3^{-}$ $CD56^{bright}$ cells is at least partially attributable to their higher trafficking capacity across the BBB. CSF subsets of NK cells differ from those in blood. The proportion of $CD3^{-}$ $CD56^{dim}$ cells was lower in the CSF, whereas $CD3^{-}$ $CD56^{bright}$ cells were overrepresented and showed an activated phenotype because they were able to degranulate more (Han et al., 2014). The enhanced presence of regulatory immune cells, such as $CD3^{-}$ $CD56^{bright}$ cells, and the reduced recruitment of $CD3^{-}$ $CD56^{dim}$ cells, limits the potential for immune-mediated destruction of CNS tissues (Han et al., 2014).

The mode of NK cell entry into the CNS and the molecules leading to this recruitment are poorly understood. This recruitment could be coordinated by CNS resident cells, such as microglia, astrocytes, and neurons, which secrete chemokines involved in NK cell migration, including CCL2, CXCL10, and CX3CL1 (Trifilo et al., 2004; Shi et al., 2011; Hansen et al., 2007; Khan et al., 2006).

In a previous study of PWH, the percentage of NK cells in the CSF was similar to our findings (Kowarik et al., 2014) however, studies on NK cells in the CSF of PWH are scarce. Patients with viral meningitis have higher NK cell counts than patients with headache or *Guillain-Barré* syndrome, MS, or HIV (Kowarik et al., 2014). NK cells display a correlation with the dysfunction of the blood–CSF barrier (Kowarik et al., 2014). The CSF NK cell $CD56^{bright}/CD56^{dim}$ ratio is increased in MS (Rodríguez-Martín et al., 2015).

NK cells were rare in the CSF of PWH and PWoH groups, although the absolute counts of CSF NK cells were significantly higher in PWH than PWoH (Ho et al., 2013). Other flow cytometry analyses of CSF and PB showed that the frequencies of $CD3^{-}$ $CD56^{+}$ and $CD3^{+}CD56^{+}$ cells did not differ between the control and PWH (Grauer et al., 2015).

NK cells are also believed to play a role in controlling HIV infection, although their role is less well-characterized (Pohlmeyer et al., 2019).

Chronic HIV infection is also associated with phenotypic changes in NK cells, including increased expression of activation markers and reduced expression of natural cytotoxic receptors (De Maria et al., 2003; Fogli et al., 2004; Mantegani et al., 2010).

Although there are reports of increased NK cell activity during viremic HIV infection (Alter et al., 2004; Eller et al., 2009), during the chronic phase of HIV infection, NK cell numbers are low in the absence of ART (Azzoni et al., 2002; Alter et al., 2005; Mantegani et al., 2010), and most have a diminished ability to perform cytolysis and secrete cytokines (Cai et al., 1990; Brenner et al., 1993; Ullum et al., 1995, 1999; Azzoni et al., 2002; De Maria et al., 2003; Mavilio et al., 2003, 2006; Fogli et al., 2004; Barker et al., 2007; Brunetta et al., 2009; Mantegani et al., 2010). With continued viral replication, the $CD3^{-}$ $CD56^{dim}$ subset previously expanded in acute infections decreased in number and function (De Maria and

Moretta, 2008). The phenotypic and functional profiles of NK cells of HIV-infected patients who have been rendered aviremic by HAART for >2 years are similar to those of healthy donors (Mavilio et al., 2003). In our study, in the CSF and PB samples of antiretroviral controlled participants (aviremic group), the proportion of PB $CD3^-$ $CD56^{dim}$ was lower than that of PWoH, whereas PB $CD3^-$ $CD56^{bright}$ was comparable in PWH and PWoH. However, in the CSF, the proportion of $CD3^-$ $CD56^{dim}$ cells in the PWH group was higher than that in the PWoH group.

In this study, secondary exploratory comparisons were performed to assess the relationship between NKT and NK cell subpopulations and HIV RNA in CSF and PB in samples categorized by the distribution of HIV RNA in both compartments.

The proportions of $CD3^+CD56^+$ and $CD3^-$ $CD56^+$ lymphocyte subpopulations in CSF or PB were comparable in PWH with unsuppressed viral load (i.e., CSF > PB and CSF < PB in viral load) and suppressed viral load in CSF and PB. This is important, as it provides evidence for CNS HIV compartmentalization and immune stimulation, even in CNS HIV-suppressed participants.

In this study, both NKT and NK cells were identified in the group with HIV infection controlled in CSF and PB (aviremic group); in fact, CSF NKT cells were present in a higher number of aviremic samples than in viremic ones. The distribution of $CD3^-$ $CD56^{dim}$ was higher in the viremic groups than in the aviremic and PWoH groups, although the difference was not statistically significant. This finding is consistent with the persistence of immune activation in the CNS reservoir. Persistent immune activation, particularly in the CNS, is involved in the neuropsychological decline of HIV patients and the development of MRI signal abnormalities despite the presence of Cart (Grauer et al., 2015). These data also indicate that it is not sufficient to only suppress the viral load below the detection level but also to inhibit virus replication, which might prevent chronic immune cell activation, similar to the findings of previous studies (Grauer et al., 2015). We found PB $CD3^-$ $CD56^{dim}$/$CD3^-$ $CD56^{brigt}$ ratio was numerically reduced in the aviremic group compared with the PWoH group due to decrease of $CD3^-$ $CD56^{dim}$, which are mature NK cells.

In this cohort, CSF $CD3^-$ $CD56^{bright}$ lymphocytes were present in one sample of PWH, the CSF $CD3^-$ $CD56^{dim}$ / CSF $CD3^-$ $CD56^{bright}$ ratio was 2.3% / 1.8%. A participant infected by HIV-1C and CNS genetic compartmentalization. The CSF sample included in this study was collected 2.5 years after the diagnosis of CSF compartmentalization and the ARV scheme was modified to a better penetration ARV scheme, with improvement of clinical symptoms (de Almeida et al., 2017). CSF $CD3^-$ $CD56^{bright}$ has a regulatory function. In neuroimmunological diseases such as MS, following several MS therapies (e.g., daclizumab or IFN-b), an expansion of regulatory $CD3^-$ $CD56^{bright}$ is observed, which is associated with a good response to treatment (Bielekova et al., 2011; Martínez-Rodríguez et al., 2011; Nabatanzi et al., 2018).

In this cohort, among the PWH, CSF predominates $CD3^-$ $CD56^{dim}$, which are effector lymphocytes, whereas in PB, the medians of $CD3^-$ $CD56^{dim}$ and $CD3^-$ $CD56^{bright}$ were greater than in the PWoH group; however, $CD3^-$ $CD56^{dim}$ predominated.

The findings of the present study provide additional support and evidence for our previously published studies that found that CSF inflammation biomarker levels were comparable between HIV-1B and HIV-1C (de Almeida et al., 2016, 2020, 2021), as well as the frequency of HAND (de Almeida et al., 2013).

The main strength of this study was that it is the first to examine NKT and NK subpopulations in the CSF and blood of PWH infected with HIV-1 subtype C, compared to HIV-negative healthy controls. All previous studies analyzed only HIV-1 subtype B. Additionally, participants with HIV-1 subtypes B and C were from the same geographical region in southern Brazil and were similar in age and HIV infection characteristics. HIV-positive and HIV-negative samples were concurrently analyzed.

This study had the following limitations: (a) The cross-sectional design limited the study; (b) PWH who were on antiretroviral treatment or untreated were enrolled, with most of the participants being on ART. We attempted to overcome this limitation by considering the plasma HIV viral load in the multivariate analysis. Nonetheless, HIV-1B and HIV-1C were found to be comparable in terms of the CSF-to-plasma HIV RNA ratio. (c) The small sample size limits the validity of some findings, especially in groups categorized according to HIV RNA in CSF and blood compartments. (d) Furthermore, the low number of events acquired in CSF samples limited the analysis mainly for $CD3^{-}$ $CD56^{dim}$ or $CD3^{-}$ $CD56^{bright}$ lymphocytes. (e) In this study $CD56^{-}$ $CD16^{+}$ cells were not investigated. Although a vast majority of NK cells can be included in the $CD3^{-}$ $CD56^{dim}$ or $CD3^{-}$ $CD56^{bright}$ groups, another subpopulation has been defined, $CD56^{-}$ $CD16^{+}$, with low cytotoxic activity and cytokine production. Chronic HIV infection leads to alterations in NK cell subset distribution, with a decline in the proportion of $CD56^{+}$ NK cells and a dramatic expansion of $CD56^{-}$ $CD16^{+}$ cells (Alter et al., 2005; Mavilio et al., 2005; Alter and Altfeld, 2009; Björkström et al., 2010; Hong et al., 2010).

5. Conclusion

The results showed compartmentalization of NKT cells in PWH, with levels being higher in the CSF than in the PB, but no differences between the HIV subtypes B and C. There was an increase in $CD3^{-}$ $CD56^{dim}$ in the CSF of PWH when compared to the PWoH group. The impact of HIV-1 *Tat* on the innate immune response is not subtype-dependent. This is the first study to evaluate NKT and NK lymphocytes in the CSF and PB of HIV-1 subtype C patients, thereby contributing to the knowledge of mechanisms underlying the pathophysiology of HIV infection in the CNS, as well as the impact of HIV-1 genetic diversity on these cells activation. However more studies are necessary due to the scarce number of these cells in CSF.

Supplementary Material

Refer to Web version on PubMed Central for supplementary material.

Source of funding

This research did not receive any specific grant from funding agencies in the public, commercial, or not-for-profit sectors.

Data availability

Data will be made available on request.

References

Albini A, Benelli R, Giunciuglio D, Cai T, Mariani G, Ferrini S, Noonan D, 1998. Identification of a novel domain of HIV tat involved in monocyte chemotaxis. J. Biol. Chem. 273, 15895–15900. [PubMed: 9632634]

Alter G, Altfeld M, 2009. NK cells in HIV-1infection: evidence for their role in the control of HIV-1infection. J. Intern. Med. 265, 29–42. [PubMed: 19093958]

Alter G, Malenfant JM, Delabre RM, Burgett NC, Yu XG, Lichterfeld M, Zaunders J, Altfeld M, 2004. Increased natural killer cell activity in viremic HIV-1 infection. J. Immunol. 173, 5305–5311. [PubMed: 15470077]

Alter G, Teigen N, Davis BT, Addo MM, Suscovich TJ, Waring MT, Streeck H, Johnston MN, Staller KD, Zaman MT, Yu XG, Lichterfeld M, Basgoz N, Rosenberg ES, Altfeld M, 2005. Sequential deregulation of NK cell subset distribution and function starting in acute HIV-1 infection. Blood 106, 3366–3369. [PubMed: 16002429]

Azzoni L, Papasavvas E, Chehimi J, Kostman JR, Mounzer K, Ondercin J, Perussia B, Montaner LJ, 2002. Sustained impairment of IFN- gamma secretion in suppressed HIV-infected patients despite mature NK cell recovery: evidence for a defective reconstitution of innate immunity. J. Immunol. 168, 5764–5770. [PubMed: 12023377]

Barker EE, Martinson JJ, Brooks CC, Landay AA, Deeks SS, 2007. Dysfunctional natural killer cells, in vivo, are governed by HIV viremia regardless of whether the infected individual is on antiretroviral therapy. AIDS 21, 2363–2365. [PubMed: 18090295]

Beall CJ, Mahajan S, Kuhn DE, Kolattukudy PE, 1996. Site-directed mutagenesis of monocyte chemoattractant protein-1 identifies two regions of the polypeptide essential for biological activity. Biochem. J. 313, 633–640. [PubMed: 8573103]

Bennasser Y, Bahraoui E, 2002. HIV-1 tat protein induces interleukin-10 in human peripheral blood monocytes, involvement of protein kinase C-beta II and -delta. FASEB J. 16, 546–554. [PubMed: 11919157]

Bielekova B, Catalfamo M, Reichert-Scrivner S, 2006. Regulatory CD56 (bright) natural killer cells mediate immunomodulatory effects of IL-2R alpha-targeted therapy (daclizumab) in multiple sclerosis. Proc. Natl. Acad. Sci. U. S. A. 103, 5941–5946. [PubMed: 16585503]

Bielekova B, Richert N, Herman ML, Ohayon J, Waldmann TA, McFarland H, Martin R, Blevins G, 2011. Intrathecal effects of daclizumab treatment of multiple sclerosis. Neurology 77, 1877–1886. [PubMed: 22076546]

Björkström NK, Ljunggren HG, Sandberg JK, 2010. CD56 negative NK cells: origin, function, and role in chronic viral disease. Trends Immunol. 31, 401–406. [PubMed: 20829113]

Bojarska-Junak A, Hus I, Sieklucka M, Wasik-Szczepanek E, Mazurkiewicz T, Polak P, Dmoszynska A, Rolinski J, 2010. Natural killer-like T CD3+CD56+ cells in chronic lymphocytic leukemia: intracellular cytokine expression and relationship with clinical outcome. Oncol. Rep. 24, 803–810. [PubMed: 20664990]

Brasil, Ministério da Saúde, 2018. Programa Nacional de DST/AIDS. http://www.aids.gov.br/assistencia/manualdst/item12.htm.

Brenner BG, Gryllis C, Gornitsky M, Wainberg MA, 1993. Changes in natural immunity during the course of HIV-1 infection. Clin. Exp. Immunol. 93, 142–148. [PubMed: 7688673]

Brunetta E, Fogli M, Varchetta S, Bozzo L, Hudspeth KL, Marcenaro E, Moretta A, Mavilio D, 2009. The decreased expression of Siglec-7 represents an early marker of dysfunctional natural killer-cell subsets associated with high levels ofHIV-1viremia. Blood 114, 3822–3830. [PubMed: 19710502]

Cai Q, Huang XL, Rappocciolo G, Rinaldo CR, 1990. Natural killer cell responses in homosexual men with early HIV infection. J. Acquir. Immune Defic. Syndr. 3, 669–676. [PubMed: 2141073]

Caligiuri MA, 2008. Human natural killer cells. Blood 112, 461–469. [PubMed: 18650461]

Chen P, Mayne M, Power C, Nath A, 1997. The tat protein of HIV-1 induces tumor necrosis factor-alpha production. Implications for HIV-1-associated neurological diseases. J. Biol. Chem. 272, 22385–22388. [PubMed: 9278385]

Conductier G, Blondeau N, Guyon A, Nahon JL, Rovère C, 2010. The role of monocyte chemoattractant protein MCP1/CCL2 in neuroinflammatory diseases. J. Neuroimmunol. 224, 93–100. [PubMed: 20681057]

Cooper MA, Fehniger TA, Caligiuri MA, 2001. The biology of human natural killer-cell subsets. Trends Immunol. 22, 633–640. [PubMed: 11698225]

Craig FE, Ohori NP, Gorrill TS, Swerdlow SH, 2011. Flow cytometric immunophenotyping of cerebrospinal fluid specimens. Am. J. Clin. Pathol. 135, 22–34. [PubMed: 21173121]

de Almeida SM, Ribeiro CE, de Pereira AP, Badiee J, Cherner M, Smith D, Maich I, Raboni SM, Rotta I, Barbosa FJ, Heaton RK, Umlauf A, Ellis RJ, 2013. Neurocognitive impairment in HIV-1 clade C- versus B-infected individuals in southern Brazil. J. Neurovirol. 19, 550–556. [PubMed: 24277437]

de Almeida SM, Rotta I, Jiang Y, Li X, Raboni SM, Ribeiro CE, Smith D, Potter M, Vaida F, Letendre S, Ellis RJ, 2016. Biomarkers of chemotaxis and inflammation in cerebrospinal fluid and serum in individuals with HIV-1 subtype C versus B. J. Neurovirol. 22, 715–724. [PubMed: 27400932]

de Almeida SM, Rotta I, Ribeiro CE, Oliveira MF, Chaillon A, de Pereira AP, Cunha AP, Zonta M, Bents JF, Raboni SM, Smith D, Letendre S, Ellis RJ, 2017. Dynamic of CSF and serum biomarkers in HIV-1 subtype C encephalitis with CNS genetic compartmentalization-case study. J. Neurovirol. 23, 460–473. [PubMed: 28247269]

de Almeida SM, Rotta I, de Pereira AP, Tang B, Umlauf A, Ribeiro CEL, Letendre S, Ellis RJ, 2020. Cerebrospinal fluid pleocytosis as a predictive factor for CSF and plasma HIV RNA discordance and escape. J. Neurovirol. 26, 241–251. [PubMed: 32002817]

de Almeida SM, Rotta I, Vidal LRR, Dos Santos JS, Nath A, Johnson K, Letendre S, Ellis RJ, 2021. HIV-1C and HIV-1B tat protein polymorphism in southern Brazil. J. Neurovirol. 27, 126–136. [PubMed: 33462791]

de Almeida SM, Beltrame MP, Tang B, Rotta I, Schluga Y, Justus JLP, da Rocha MT, Abramson I, Vaida F, Schrier R, Ellis RJ, 2022. Main lymphocyte subpopulations in cerebrospinal fluid and peripheral blood in HIV-1 subtypes C and B. J. Neurovirol. 28, 291–304. [PubMed: 35190973]

de Graaf MT, Smitt PA, Luitwieler RL, van Velzen C, van den Broek PD, Kraan J, Gratama JW, 2011. Central memory CD4+ T cells dominate the normal cerebrospinal fluid. Cytometry B Clin. Cytom. 80, 43–50. [PubMed: 20632412]

De Maria A, Moretta L, 2008. NK cell function in HIV-1 infection. Curr. HIV Res. 6, 433–440. [PubMed: 18855653]

De Maria A, Fogli M, Costa P, Murdaca G, Puppo F, Mavilio D, Moretta A, Moretta L, 2003. The impaired NK cell cytolytic function in viremic HIV-1 infection is associated with a reduced surface expression of natural cytotoxicity receptors (NKp46,NKp30and NKp44). Eur. J. Immunol. 33, 2410–2418. [PubMed: 12938217]

Elewaut D, Kronenberg M, 2000. Molecular biology of NK T cell specificity and development. Semin. Immunol. 12, 561–568. [PubMed: 11145862]

El-Hagrasy HA, Hassanein N, 2019. Evaluation of NK and TNK cells in peripheral blood of adult patients with benign lymphocytosis. Clin. Med. Diag. 9, 1–7.

Eller MA, Eller LA, Ouma BJ, Thelian D, Gonzalez VD, Guwatudde D, McCutchan FE, Marovich MA, Michael NL, de Souza MS, Wabwire-Mangen F, Robb ML, Currier JR, Sandberg JK, 2009. Elevated natural killer cell activity despite altered functional and phenotypic profile in Ugandans with HIV-1 clade A or clade D infection. J. Acquir. Immune Defic. Syndr. 51, 380–389. [PubMed: 19487954]

Fleuridor R, Wilson B, Hou R, Landay A, Kessler H, Al-Harthi L, 2003. CD1d restricted natural killer T cells are potent targets for human immunodeficiency virus infection. Immunology 108, 3–9. [PubMed: 12519296]

Fogli M, Costa P, Murdaca G, Setti M, Mingari MC, Moretta L, Moretta A, De Maria A, 2004. Significant NKcell activation associated with decreased cytolyticf unction in peripheral blood of HIV-1-infected patients. Eur. J. Immunol. 34, 2313–2321. [PubMed: 15259029]

Grauer OM, Reichelt D, Grüneberg U, Lohmann H, Schneider-Hohendorf T, Schulte-Mecklenbeck A, Gross CC, Meuth SG, Wiendl H, Husstedt IW, 2015. Neurocognitive decline in HIV patients is associated with ongoing T-cell activation in the cerebrospinal fluid. Ann. Clin. Transl. Neurol. 2, 906–919. [PubMed: 26401512]

Gross CC, Schulte-Mecklenbeck A, Rünzi A, Kuhlmann T, Posevitz-Fejfár A, Schwab N, Schneider-Hohendorf T, Herich S, Held K, Konjevic M, Hartwig M, Dornmair K, Hohlfeld R, Ziemssen T, Klotz L, Meuth SG, Wiendl H, 2016. Impaired NK-mediated regulation of T-cell activity in multiple sclerosis is reconstituted by IL-2 receptor modulation. Proc. Natl. Acad. Sci. U. S. A. 113, E2973–E2982. [PubMed: 27162345]

Gross CC, Pawlitzki M, Schulte-Mecklenbeck A, Rolfes L, Ruck T, Hundehege P, Wiendl H, Herty M, Meuth SG, 2020. Generation of a model to predict differentiation and migration of lymphocyte subsets under homeostatic and CNS autoinflammatory conditions. Int. J. Mol. Sci. 21, 2046. [PubMed: 32192056]

Hamann I, Dörr J, Glumm R, Chanvillard C, Janssen A, Millward JM, Paul F, Ransohoff RM, Infante-Duarte C, 2013. Characterization of natural, killer cells in paired CSF and blood samples during neuroinflammation. J. Neuroimmunol. 254, 165–169. [PubMed: 22948090]

Han S, Lin YC, Wu T, Salgado AD, Mexhitaj I, Wuest SC, Romm E, Ohayon J, Goldbach-Mansky R, Vanderver A, Marques A, Toro C, Williamson P, Cortese I, Bielekova B, 2014. Comprehensive immunophenotyping of cerebrospinal fluid cells in patients with neuroimmunological diseases. J. Immunol. 192, 2551–2563. [PubMed: 24510966]

Hansen DS, Bernard NJ, Nie CQ, Schofield L, 2007. NK cells stimulate, recruitment of CXCR3+ T cells to the brain during plasmodium berghei-mediated, cerebral malaria. J. Immunol. 178, 5779–5788. [PubMed: 17442962]

Ho EL, Ronquillo R, Altmeppen H, Spudich SS, Price RW, Sinclair E, 2013. Cellular composition of cerebrospinal fluid in HIV-1 infected and uninfected subjects. PLoS One 18, 8 (6), e66188.

Hong HS, Eberhard JM, Keudel P, Bollmann BA, Ahmad F, Ballmaier M, Bhatnagar N, Zielinska-Skowronek M, Schmidt RE, Meyer-Olson D, 2010. Phenotypically and functionally distinct subsetsc ontribute to the expansion of CD56−/CD16+ natural killer cells in HIV infection. AIDS 24, 1823–1834. [PubMed: 20543659]

Hu PF, Hultin LE, Hultin P, Hausne RMA, Hirji K, Jewett A, Bonavida B, Detels R, Giorgi JV, 1995. Natural killer cell immunodeficiency in HIV disease is manifest by profoundly decreased numbers of CD16+ CD56+ cells and expansion of a population of CD16dim CD56- cells with low lytic activity. J. Acquir. Immune Defic. Syndr. Hum. Retrovirol. 10, 331–340. [PubMed: 7552495]

Huang D, Shi FD, Jung S, 2006. The neuronal chemokine CX3CL1/ fractalkine selectively recruits NK cells that modify experimental autoimmune encephalomyelitis within the central nervous system. FASEB J. 20, 896–905. [PubMed: 16675847]

Khan IA, Thomas SY, Moretto MM, 2006. CCR5 is essential for NK cell trafficking and host survival following *Toxoplasma gondii* infection. PLoS Pathog. 2, e49. [PubMed: 16789839]

Kim CH, Butcher EC, Johnston B, 2002. Distinct subsets of human Vα24-invariant NKT cells: cytokine responses and chemokine receptor expression. Trends Immunol. 23, 516–519. [PubMed: 12401396]

Kowarik MC, Grummel V, Wemlinger S, Buck D, Weber MS, Berthele A, Hemmer B, 2014. Immune cell subtyping in the cerebrospinal fluid of patients with neurological diseases. J. Neurol. 261, 130–143. [PubMed: 24162037]

Krijgsman D, de Vries NL, Skovbo A, Andersen MN, Swets M, Bastiaannet E, Vahrmeijer AL, van de Velde CJH, Heemskerk MHM, Hokland M, Kuppen PJK, 2019. Characterization of circulating T-, NK-, and NKT cell subsets in patients with colorectal cancer: the peripheral blood immune cell profile. Cancer Immunol. Immunother. 68, 1011–1024. [PubMed: 31053876]

Kutsch O, Oh J, Nath A, Benveniste EN, 2000. Induction of the chemokines interleukin-8 and IP-10 by human immunodeficiency virus type 1 tat in astrocytes. J. Virol. 74, 9214–9221. [PubMed: 10982368]

Lanier LL, Le AM, Civin CI, Loken MR, Phillips JH, 1986. The relationship of CD16 (Leu-11) and Leu-19 (NKH–1) antigen expression on human peripheral blood NK cells and cytotoxic T lymphocytes. J. Immunol. 136, 4480–4486. [PubMed: 3086432]

Letendre SL, FitzSimons C, Ellis RJ, Clifford D, Collier AC, Gelman B, Marra C, McArthur J, McCutchan JA, Morgello S, Simpson D, Vaida F, Heaton R, Grant I, 2010. Correlates of CSF viral loads in 1,221 volunteers of the CHARTER cohort. In: Program and Abstracts of the 17th Conference on Retroviruses and Opportunistic Infections; San Francisco, CA (poster 430).

Mantegani P, Tambussi G, Galli L, Din CT, Lazzarin A, Fortis C, 2010. Perturbation of the natural killer cell compartment during primary human immunodeficiency virus1infection primarily involving the CD56 bright subset. Immunology 129, 220–233. [PubMed: 19824914]

Martínez-Rodríguez JE, Lo'pez-Botet M, Munteis E, Rio J, Roquer J, Montalban X, Comabella M, 2011. Natural killer cell phenotype and clinical response to interferon-beta therapy in multiple sclerosis. Clin. Immunol. 141, 348–356. [PubMed: 21992960]

Mavilio D, Benjamin J, Daucher M, Lombardo G, Kottilil S, Planta MA, Marcenaro E, Bottino C, Moretta L, Moretta A, Fauci AS, 2003. Natural killer cells in HIV-1infection: dichotomous effects of viremia on inhibitory and activating receptors and their functional correlates. Proc. Natl. Acad. Sci. U. S. A. 100, 15011–15016. [PubMed: 14645713]

Mavilio D, Lombardo G, Benjamin J, Kim D, Follman D, Marcenaro E, O'Shea MA, Kinter A, Kovacs C, Moretta A, Fauci AS, 2005. Characterization of CD56−/CD16+ natural killer (NK) cells: a highly dysfunctional NK subset expanded in HIV-infected viremic individuals. Proc. Natl. Acad. Sci. U. S. A. 102, 2886–2891. [PubMed: 15699323]

Mavilio D, Lombardo G, Kinter A, Fogli M, La Sala A, Ortolano S, Farschi A, Follmann D, Gregg R, Kovacs C, Marcenaro E, Pende D, Moretta A, Fauci AS, 2006. Characterization of the defective interaction between a subset of natural killer cells and dendritic cells in HIV-1 infection. J. Exp. Med. 203, 2339–2350. [PubMed: 17000867]

Mayo L, Quintana FJ, Weiner HL, 2012. The innate immune system in demyelinating disease. Immunol. Rev. 248, 170–187. [PubMed: 22725961]

Michel T, Poli A, Cuapio A, Briquemont B, Iserentant G, Ollert M, Zimmer J, 2016. Human CD56bright NK cells: an update. J. Immunol. 196, 2923–2931. [PubMed: 26994304]

Milush JM, López-Ver ès S, York VA, Deeks SG, Martin JN, Hecht FM, Lanier LL, Nixon DF, 2013. CD56neg CD16(+) NK cells are activated mature NK cells with impaired effector function during HIV-1 infection. Retrovirology 10, 158. [PubMed: 24351015]

Monteiro de Almeida S, Letendre S, Zimmerman J, Lazzaretto D, McCutchan A, Ellis R, 2005. Dynamics of monocyte chemoattractant protein type one (MCP-1) and HIV viral load in human cerebrospinal fluid and plasma. J. Neuroimmunol. 169, 144–152. [PubMed: 16182380]

Moretta L, 2010. Dissecting CD56dim human NK cells. Blood 116, 3689–3691. [PubMed: 21071612]

Moretta A, Marcenaro E, Parolini S, Ferlazzo G, Moretta L, 2008. NK cells at the interface between innate and adaptive immunity. Cell Death Differ. 15, 226–233. [PubMed: 17541426]

Motsinger A, Haas DW, Stanic AK, Van Kaer L, Joyce S, Unutmaz D, 2002. CD1d restricted human natural killer T cells are highly susceptible to human immunodeficiency virus 1 infection. J. Exp. Med. 195, 869–879. [PubMed: 11927631]

Nabatanzi R, Cose S, Joloba M, Jones SR, Nakanjako D, 2018. Effects of HIV infection and ART on phenotype and function of circulating monocytes, natural killer, and innate lymphoid cells. AIDS Res. Ther. 15, 7. [PubMed: 29544508]

Nguyen MD, Julien JP, Rivest S, 2002. Innate immunity: the missing link in neuroprotection and neurodegeneration? Nat. Rev. Neurosci. 3, 216–227. [PubMed: 11994753]

Olteanu H, Schur BC, Bredeson C, Atallah E, Kroft SH, 2010. Expression of natural killer receptors in T and NK-cells: comparison of healthy individuals, patients with prior stem cell transplant, and patients undergoing chemotherapy. Leuk. Lymphoma 51, 481–487. [PubMed: 20141431]

Poggi A, Carosio R, Spaggiari GM, Fortis C, Tambussi G, Dell'Antonio G, Dal Cin E, Rubartelli A, Zocchi MR, 2002. NK cell activation by dendritic cells is dependent on LFA-1-mediated induction

of calcium-calmodulin kinase II: inhibition by HIV-1 tat C-terminal domain. J. Immunol. 168, 95–101. [PubMed: 11751951]

Pohlmeyer CW, Gonzalez VD, Irrinki A, Ramirez RN, Li L, Mulato A, Murry JP, Arvey A, Hoh R, Deeks SG, Kukolj G, Cihlar T, Pflanz S, Nolan GP, Min-Oo G, 2019. Identification of NK cell subpopulations that differentiate HIVinfected subject cohorts with diverse levels of virus control. J. Virol. 93 e01790–18. [PubMed: 30700608]

Poli A, Michel T, Theresine M, Andres E, Hentges F, Zimmer J, 2009. CD56bright natural killer (NK) cells: an important NK cell subset. Immunology 126, 458–465. [PubMed: 19278419]

Quijano S, López A, Sancho JM, Panizo C, Debén G, Castilla C, García-Vela JA, Salar A, Alonso-Vence N, González-Barca E, Peñalver FJ, Plaza-Villa J, Morado M, García-Marco J, Arias J, Briones J, Ferrer S, Capote J, Nicolás C, Orfao A, 2009. Identification of leptomeningeal disease in aggressive B-cell non-Hodgkin's lymphoma: improved sensitivity of flow cytometry. J. Clin. Oncol. 27, 1462–1469. [PubMed: 19224854]

Ranga U, Shankarappa R, Siddappa NB, Ramakrishna L, Nagendran R, Mahalingam M, Mahadevan A, Jayasuryan N, Satishchandra P, Shankar SK, Prasad VR, 2004. Tat protein of human immunodeficiency virus type 1 subtype C strains is a defective chemokine. J. Virol. 78, 2586–2590. [PubMed: 14963162]

Raulet DH, 2003. Roles of the NKG2D immunoreceptor and its ligands. Nat. Ver. Immunol. 3, 781–790.

Rodríguez-Martín E, Picón C, Costa-Frossard L, Alenda R, Sainz de la Maza S, Roldán E., Espiño M., Villar LM., Álvarez-Cermeño JC., 2015. Natural killer cell subsets in cerebrospinal fluid of patients with multiple sclerosis. Clin. Exp. Immunol. 180, 243–249. [PubMed: 25565222]

Ruhanya V, Jacobs GB, Naidoo S, Paul RH, Joska JA, Seedat S, Nyandoro G, Engelbrecht S, Glashof RH, 2021. Impact of plasma IP-10/CXCL10 and RANTES/CCL5 levels on neurocognitive function in HIV treatment-naive patients. AIDS Res. Hum. Retrovir. 7, 657–665.

Shi FD, Ljunggren HG, La Cava A, Van Kaer L, 2011. Organ-specific features of natural killer cells. Nat. Rev. Immunol. 11, 658–671. [PubMed: 21941294]

Slauenwhite D, Johnston B, 2015. Regulation of NKT cell localization in homeostasis and infection. Front. Immunol. 6, 255. [PubMed: 26074921]

Svenningsson A, Hansson GK, Andersen O, Andersson R, Patarroyo M, Stemme S, 1993. Adhesion molecule expression on cerebrospinal fluid T lymphocytes: evidence for common recruitment mechanisms in multiple sclerosis, aseptic meningitis, and normal controls. Ann. Neurol. 34, 155–161. [PubMed: 8338339]

Svenningsson A, Andersen O, Edsbagge M, Stemme S, 1995. Lymphocyte phenotype and subset distribution in normal cerebrospinal fluid. J. Neuroimmunol. 63, 39–46. [PubMed: 8557823]

Taborda NA, Hernández JC, Montoya CJ, Rugeles MT, 2014. Las células natural killer y su papel en la respuesta inmunitaria durante la infección por el virus de la inmunodeficiencia humana tipo-1. Inmunología 33, 11–20.

Tarazona R, Dela Rosa O, Alonso C, Ostos B, Espejo J, Peña J, Solana R, 2000. Increased expression of NK cell markers on T lymphocytes in aging and chronic activation of the immune system reflects the accumulation of effector/senescent T cells. Mech. Ageing Dev. 121, 77–88. [PubMed: 11164462]

Tomescu C, Abdulhaqq S, Montaner LJ, 2011. Evidence for the innate immune response as a correlate of protection in human immunodeficiency virus (HIV)-1 highly exposed seronegative subjects (HESN). Clin. Exp. Immunol. 164, 158–169. [PubMed: 21413945]

Trifilo MJ, Montalto-Morrison C, Stiles LN, Hurst KR, Hardison JL, Manning JE, Masters PS, Lane TE, 2004. CXC chemokine ligand 10 controls viral infection in the central nervous system: evidence for a role in innate immune response through recruitment and activation of natural killer cells. J. Virol. 78, 585–594. [PubMed: 14694090]

Trinchieri G, 1989. Biology of natural killer cells. Adv. Immunol. 46, 181.

Uemura Y, Suzuki M, Liu TY, Narita Y, Hirata S, Ohyama H, Ishihara O, Matsushita S, 2008. Role of human non-invariant NKT lymphocytes in the maintenance of type 2T helper environment during pregnancy. Int. Immunol. 20, 405–412. [PubMed: 18234691]

Ullum HH, Gøtzsche PCP, Victor JJ, Dickmeiss EE, Skinhøj PP, Pedersen BKB, 1995. Defective natural immunity: a nearly manifestation of human immunodeficiency virus infection. J. Exp. Med. 182, 789–799. [PubMed: 7650485]

Ullum H, Cozzi Lepri A, Aladdin H, Katzenstein T, Victor J, Phillips AN, Gerstoft J, Skinhøj P, Klarlund Pedersen B, 1999. Natural immunity and HIV disease progression. AIDS 13, 557–563. [PubMed: 10203380]

Williams ME, Zulu SS, Stein DJ, Joska JA, Naudé PJW, 2020. Signatures of HIV-1 subtype B and C tat proteins and their effects in the neuropathogenesis of HIV-associated neurocognitive impairments. Neurobiol. Dis. 136, 104701. [PubMed: 31837421]

Zhou J, Zhao X, Wang Z, Wang J, Sun H, Hu Y, 2013. High circulating CD3+ CD56+CD16+ natural killer-like T cell levels predict a better IVF treatment outcome. J. Reprod. Immunol. 97, 197–203. [PubMed: 23452704]

Zipeto D, Serena M, Mutascio S, Parolini F, Diani E, Guizzardi E, Muraro V, Lattuada E, Rizzardo S, Malena M, Lanzafame M, Malerba G, Romanelli MG, Tamburin S, Gibellini D, 2018. HIV1-associated neurocognitive disorders: is HLA-C binding stability to β2-microglobulin a missing piece of the pathogenetic puzzle? Front. Neurol. 9, 791. [PubMed: 30298049]

Zocchi MR, Rubartelli A, Morgavi P, Poggi A, 1998. HIV-1 tat inhibits human natural killer cell function by blocking L-type calcium channels. J. Immunol. 161, 2938–2943. [PubMed: 9743356]

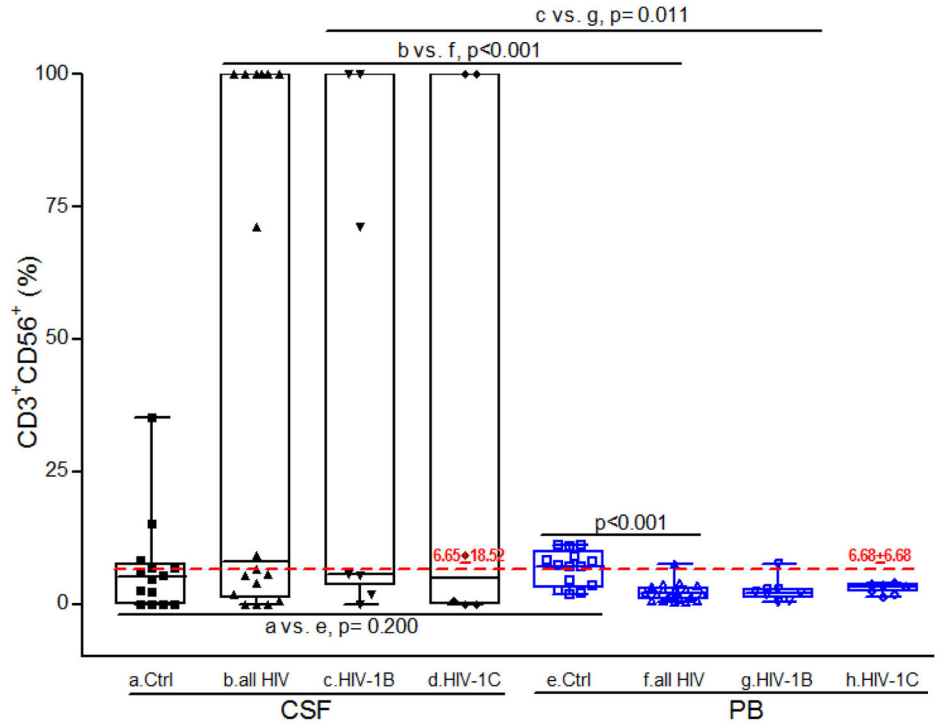

a.

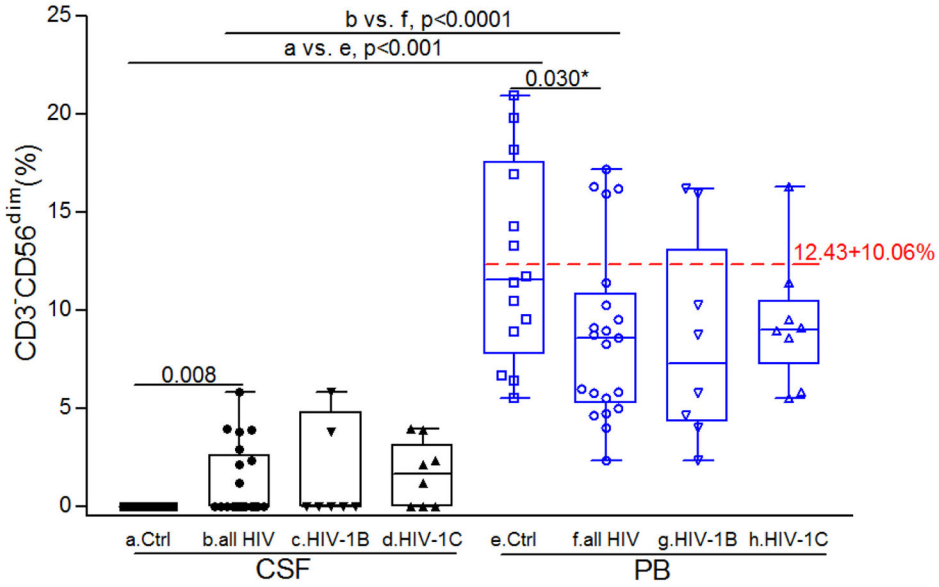

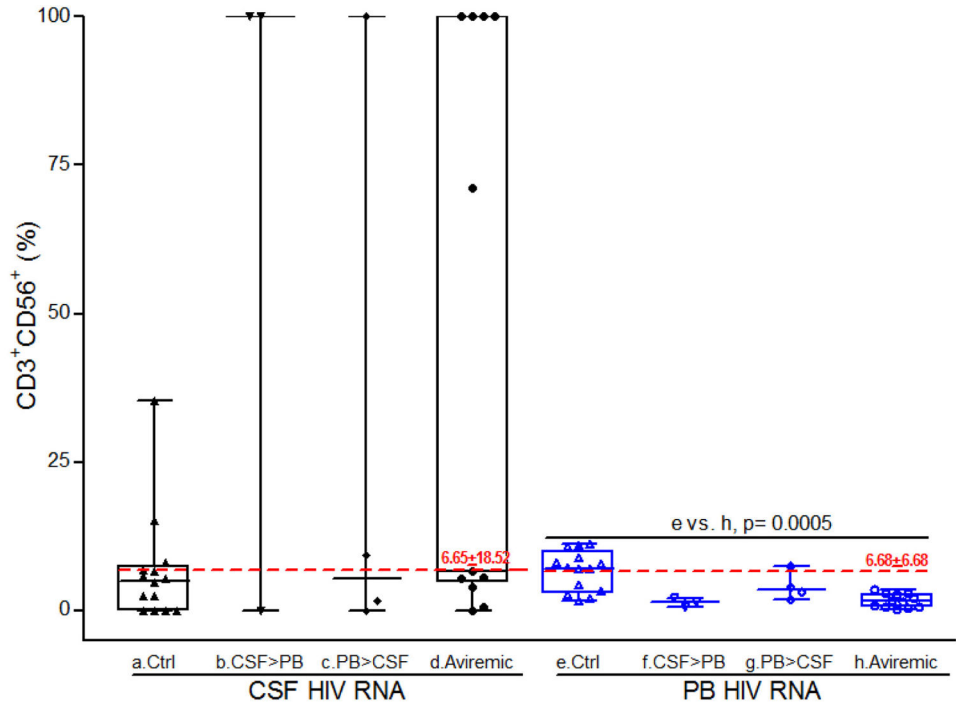

c.

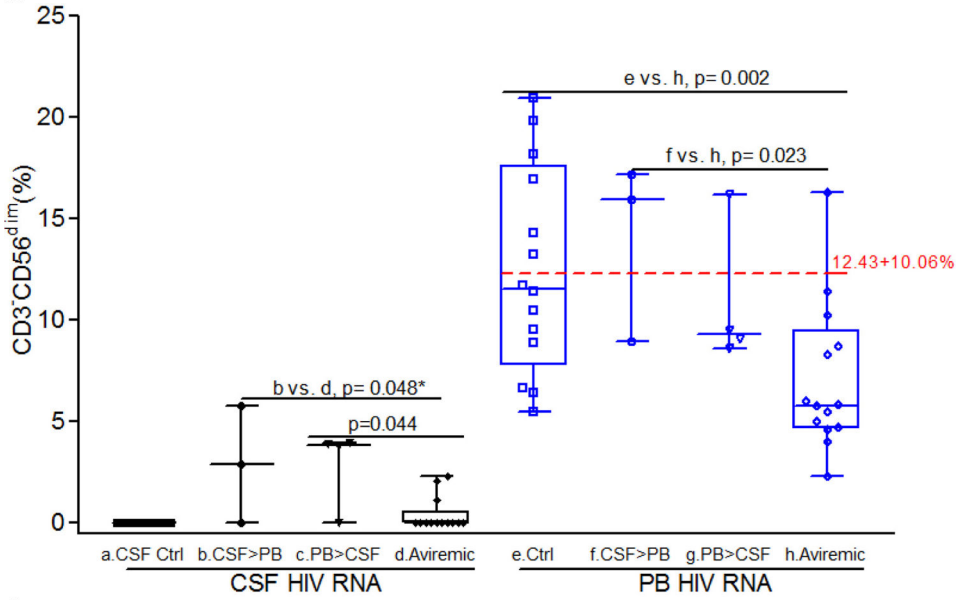

d.

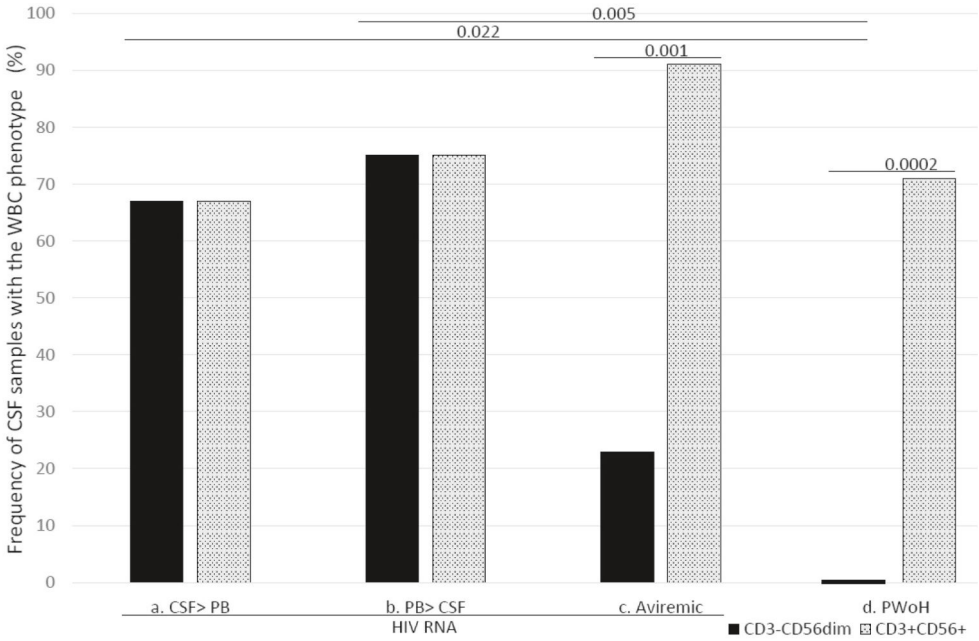

e.

Fig. 1.

Proportion of $CD3^{+}CD56^{+}$ and $CD3^{-}$ $CD56^{dim}$ lymphocytes in gated *CD45* in CSF (black) and peripheral blood (blue) by HIV serostatus and HIV-1 subtype. From a) to d), the box plots represent the medians and interquartile ranges, whiskers represent the maximum and minimum values, and dots represent individuals. The red dashed lines indicate mean ± two standard deviation in the HIV negative control group. *a)* $CD3^{+}CD56^{+}$ *and b)* $CD3^{-}$ $CD56^{dim}$ *were compared between PWH and PWoH, HIV-1 subtypes B and C, and plasma and CSF. *p = 0.060 after multiple testing correction using Benjamini Hochberg method. c)* $CD3^{+}CD56^{+}$ *and d)* $CD3^{-}$ $CD56^{dim}$ *were compared between the groups categorized according to* the HIV RNA in CSF and peripheral blood compartments. **p = 0.11 after* adjusting for multiple comparisons *with Tukey's HSD test.* e) the frequency of CSF samples $CD3^{-}$ $CD56^{dim}$ *(black)* and $CD3^{+}CD56^{+}$ (gray) lymphocytes between the groups *categorized according with* the HIV RNA in CSF and blood compartments. Ctrl, HIV negative control group. (For interpretation of the references to color in this figure legend, the reader is referred to the web version of this article.)

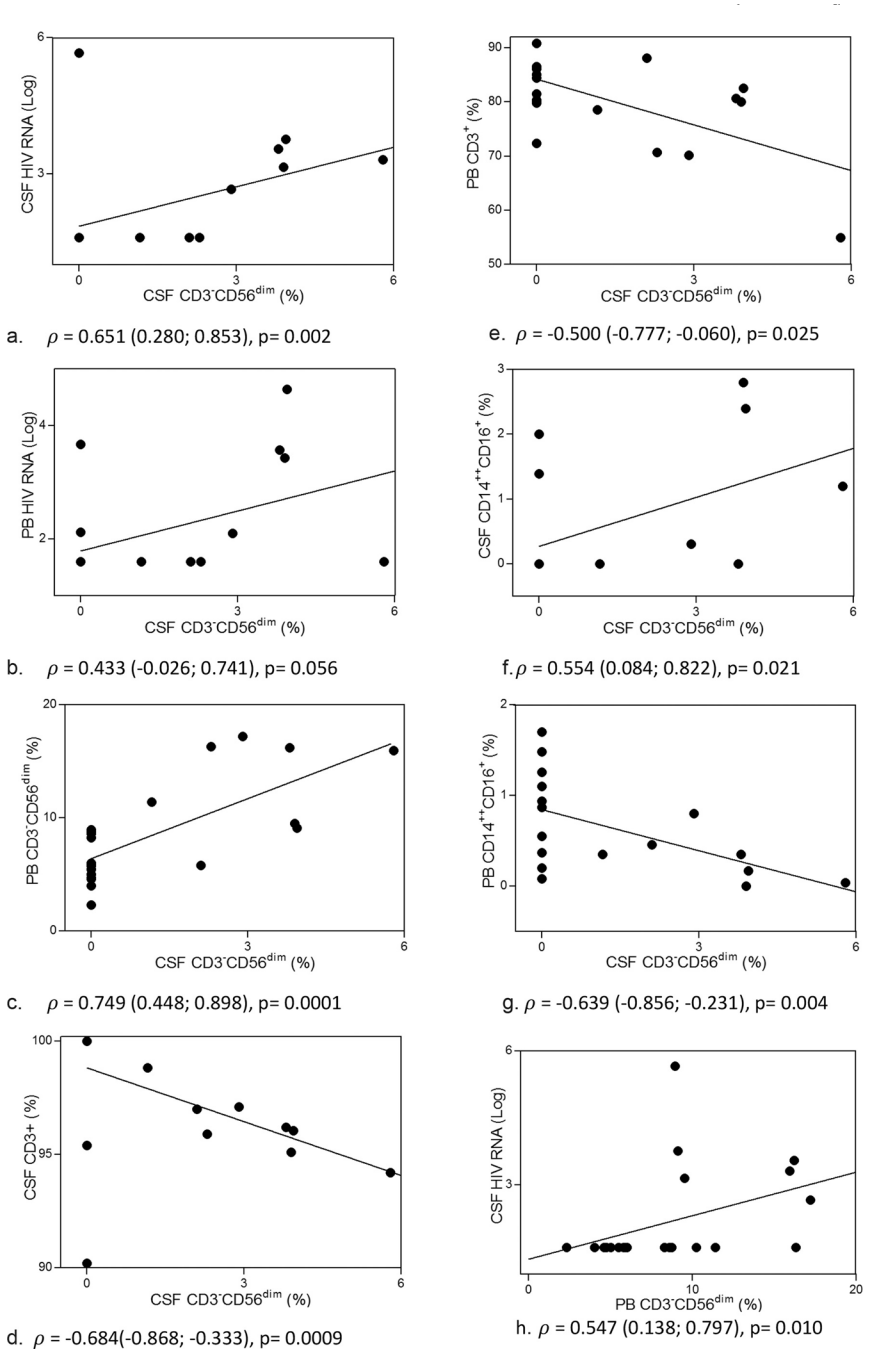

Fig. 2.

Scatterplots of correlations between biomarkers in CSF and PB. Correlation coefficients (ρ, 95% confidence intervals) estimated using Spearman's rank-order method.

Table 1

Demographic, HIV infection, and CSF characteristics of PWH and PWoH.

	all HIV+ (*n* = 22)	**HIV- (*n* = 14)**	***P***	**B (*n* = 8)**	**C (n = 9)**	***P***
Age, years	43.5 (40; 50)	43 (35.5; 52.5)	0.987	43 (41; 48.50)	43 (39.50; 54)	0.743
Male, n (%)	14 (63.64)	5 (37.71)	0.171	8 (100)	3 (33.3)	0.009
AIDS, n (%)	15 (68.18)	-	-	6 (75)	5 (55.56)	0.620
Duration, months	153 (64.97; 182.5)	-	-	156.7 (94.48; 159.70)	150.0 (67.08; 184.50)	0.481
Nadir CD4, cells/mm^3	219 (32.5; 531.5)	-	-	92.00 (26.00; 675.00)	138.0 (26.50; 800.50)	0.805
Current CD4, cells/mm^3	487 (403; 722)	-	-	637.6 (454.2; 797.1)	403.3 (326.7; 438.7)	0.065
Current CD8, cells/mm^3	825 (705; 1571)	-	-	838.5 (716.0; 1259.0)	761.0 (688.0; 1665.0)	0.867
CD4 recovery, cells/mm^3	359 (−34.30; 670)	-	-	326.8 (53.20; 982.60)	359.4 (−27.35; 587.20)	0.535
on CART, n (%)	15 (68.18)	-	-	6 (75.0)	5 (55.56)	0.620
CPE	6 (6; 8)	-	-	7 (6; 9)	6	0.537
Log_{10} Plasma HIV RNA	1.60 (1.60; 2.55)	-	-	1.6 (1.6; 1.6)	2.12 (1.60; 3.55)	0.281
Plasma HIV RNA < 50 copies/mL, n (%)	14 (63.64)	-	-	7 (87.50)	4 (44.44)	0.131
CSF, n	20	14	-	7	8	-
WBC, cells/mm^3	2.80 (1.20; 6.55)	1.75 (0.6; 2.5)	0.128	1.20 (0.60; 6.85)	4.80 (2.00; 17.80)	0.121
WBC count > 5 cells/mm^3, n (%)	6 (30)	0	0.031	1 (14.3)	4 (50)	0.282
Glucose, mg/dL	57.5 (53; 61.0)	59.5 (54.0; 64.5)	0.473	60.00 (59.00; 69.00)	53.00 (50.00; 56.50)	0.040[a]
Total protein, mg/dL	36.25 (28.90; 43.55)	30.55 (27.35; 31.75)	0.034	42.00 (40.65; 54.55)	28.90 (24.80; 39.90)	0.072
Total protein > 45 mg/dL, n(%)	4 (20)	0	0.126	2 (28.60)	2 (25)	1
Lactic acid, mmol/L	1.4 (1.3; 1.65)	1.4 (1.1; 1.5)	0.432	1.3	1.65 (1.30; 1.70)	-
RBC, cells/mm^3	0.45 (0.3; 3.75)	2.7 (0.3; 12.6)	0.344	0.60 (0.30; 7.50)	1.75 (0.15; 101.70)	0.613
Log_{10} CSF HIV RNA	1.6 (1.6; 2.91)	-	-	1.6 (1.6; 2.46)	1.6 (1.6; 3.46)	0.694
CSF HIV RNA < 50copies/mL, n (%)	13 (65)	-	-	5 (62.5)	4 (44.4)	0.608
HIV RNA CSF > blood, n (%)	3 (15)	-	-	1 (14.3)	1 (12.5)	1

CART = combination anti-retroviral therapy; CPE = anti-retroviral CNS Penetration effectiveness rank (Letendre et al., 2010); WBC, white blood cell; RBC, red blood cell.

[a]CSF glucose was significantly higher in HIV-1 subtype B than C, but in both groups CSF glucose levels were under reference range.

Table 2

Comparing proportions of $CD3^{+}CD56^{+}$ and $CD3^{-}CD56^{+}$ subsets in gate CD45 in CSF and peripheral blood between the PWH and PWoH groups.

	A-PWH	B-PWoH	Cohen's d	A vs. B	C- PWH	D- PWoH	Cohen's d	C vs. D	A vs. C	B vs. D
	(*n* = 20)	(n = 14)	(95% CI)	p	(n = 22)	(n = 14)	(95% CI)	p	p	p
	CSF				Peripheral blood					
$CD3^{+}CD56^{+}$	7.95 (1.18; 100.0)	5.05 (0.00; 7.55)	0.70 (− 0.41; 1.80)	0.210	2.00 (0.76; 3.03)	7.10 (3.00; 9.90)	− 1.96 (− 2.73. 1.19)	<0.001	<0.001	0.200
$CD3^{-}CD56^{+}$(NK total)	0.00 (0.00; 3.35)	0.00 (0.00; 0.00)	1.88 (0.65; 3.12)	0.016	8.68 (5.54; 11.80)	12.16 (8.22; 18.15)	− 0.83 (− 1.50; − 0.16)	0.021/ 0.060 *b*	<0.001	<0.001
CD3 $CD56^{dim}$	0.00 (0.00; 2.60)	0.00 (0.00; 0.00)	0.99 (0.31; 1.68)	0.008	8.59 (5.24; 10.82)	11.57 (7.76; 17.56)	− 0.78 (− 1.46; − 0.11)	0.030/ 0.060 *b*	< 0.001	<0.001
CD3-$CD56^{bright}$	0.00 (0.00; 1.80)*a*	0.00 (0.00; 0.00)	-	-	0.31 (0.23; 0.72)	0.69 (0.42; 0.91)	− 0.56 (− 1.23; 0.12)	0.16	< 0.001	<0.001
$CD56^{dim}$/ CD56bright *(c)*	0.00 (0.00; 1.28)*a*	0.00 (0.00; 0.00)	-	-	17.15 (11.92; 39.43)	18.51 (10.53; 35.22)	0.09 (− 0.58; 0.77)	0.79	<0.001	<0.001

Values represent median (IQR) or

(a) median (range).

In the comparison between HIV+ and HIV-, *p* value was adjusted for age and gender in the adjusted model, and then corrected for multiple testing with the BH method within CSF and blood and cell subtype separately; all *p*-values were corrected for multiple testing using the BH method;

(b) *p*-values before and after the BH correction. Group differences are presented as Cohen's d; CI, confidence interval; the Cohen's d (95%CI) effect sizes for the comparisons between blood and CSF (A vs. C and B vs. D) are shown in Supplementary Table 1;

(c) effector / regulatory ratio.

Table 3

Comparing proportions of $CD3^{+}CD56^{+}$ and CD3~$CD56^{+}$ subsets in gate CD45 in CSF and peripheral blood between HIV subtypes B and C groups.

	A. HIV1-B (*n* = 7)	B. HIV1-C (n = 8)	Cohen's d (95%CI)	A vs. B p	C. HIV1-B (n = 8)	D. HIV1-C (n = 9)	Cohen's d (95%CI)	C vs. D p	A vs. C p	B vs. D p
	CSF				Peripheral blood					
$CD3^{+}CD56^{+}$	5.70 (3.550; 100.0)	4.98 (0.0; 100.0)	− 0.88 (−2.03, 0.27)	0.12	2.15 (1.15; 2.84)	3.21 (2.24; 3.78)	0.19 [− 1.12, 1.51]	0.75	0.016	0.36
$CD3^{-}CD56^{+}$ (total NK)	0.0 (0.0; 4.80)	1.63 (0.00; 3.92)	0.44 (− 0.58, 1.45)	0.63	7.81 (4.84; 13.73)	9.35 (7.19; 11.22)	0.25 (− 0.93, 1.43)	0.92	< 0.001	0.003
$CD3^{-}CD56^{dim}$	0.0 (0.0; 4.80)	1.63 (0.00; 3.10)	0.39 (− 0.63; 1.40)	0.63	7.26 (4.30; 13.09)	9.03 (7.21; 10.45)	0.21 (− 0.77; 1.19)	0.92	< 0.001	0.003
$CD3^{-}CD56^{bright}$	0.0 (0.0; 0.00)	0.00 (0.00; 1.80)[a]	-	-	0.46 (0.22; 0.73)	0.37 (0.29; 0.97)	0.34 (− 0.64; 1.32)	0.92	-	<0.001
$CD56^{dim}/CD56^{bright}$	0.0 (0.0; 0.00)	0.00 (0.00; 1.28)[a]	-	-	13.39 (11.92; 51.38)	17.71 (10.85; 28.15)	− 0.05 (− 1.03; 0.93)	0.92	-	<0.001

The values are median (IQR) or

[a] median (range). p-value was adjusted for plasma HIV viral load suppression and nadir CD4 count in the comparison of HIV-1B and HIV-1C but not adjusted for covariates in the paired comparison between CSF and blood (A vs. C and B vs. D); all *p*-values were corrected for multiple testing using the BH method. Group difference is presented as Cohen's d; CI, confidence interval. The Cohen's d (95%CI) effect size for the comparisons of group A vs. C and B vs. D are shown in Supplementary Table 1.

Table 4

Proportion of $CD3^{+}CD56^{+}$ and CD3~$CD56^{+}$ lymphocytes in gate *CD45*, in CSF and peripheral blood by groups categorized according to the distribution of plasma and CSF HIV RNA.

	A- CSF > PB (n = 3)*	B- PB > CSF (n = 4)*	C- Aviremic (*n* = 13)	p*a*	C vs. Ctrl p*b*	D- CSF > PB (n = 3)*	*E*- PB > CSF (n = 4)*	F- Aviremic (n = 14)	p*a*	F vs. Ctrl p*b*
	CSF					Peripheral blood				
$CD3^{+}CD56^{+}$	100.0 (0.00; 100.0)*	5.50 (0.00; 100.0)*	6.60 (4.70; 100.0)	0.775	0.112	1.38 (0.62;2.17)	3.57 (1.87; 7.57)*	1.58 (0.540; 2.71)	0.070	0.0005
$CD3^{-}CD56^{+}$ (total NK)	2.90 (0.00; 5.80)*	3.85 (0.00; 3.94)*	0.0 (0.00; 0.58)	0.074	-	16.36 (9.35; 17.37)	9.86 (8.80; 16.45)	6.14 (5.02; 10.22)	0.043	0.003
$CD3^{-}CD56^{dim}$	2.90 (0.00; 5.80)	3.85 (0.00; 3.94)	0.00 (0.00; 0.58)	0.023	-	15.94 (8.95; 17.20)	9.30 (8.59; 16.20)	5.81 (4.66; 9.49)	0.035	0.002
$CD3^{-}CD56^{bright}$	0.00 (0.00; 0.00)	0.00 (0.00; 0.00)	0.00 (0.00; 1.80)*	0.764	-	0.40 (0.17; 0.42)	0.27 (0.21; 0.84)	0.33 (0.24; 0.93)	0.673	0.206
$CD56^{dim}/CD56^{bright}$	0.00 (0.00; 0.00)	0.00 (0.00; 0.00)	0.00 (0.00; 1.28)*	-	-	37.95 (22.38; 101.20)	37.42 (10.83; 64.80)	14.49 (11.33; 23.92)	0.105	0.535

Values represent the median (IQR) or

*median (range); Ctrl = the control group.

Pairwise comparison (Mann-Whitney) for peripheral blood $CD3^{-}CD56^{+}$ (total NK): D vs. E, $p = 0.629$; D vs. F, $p = 0.051$; E vs. F, $p = 0.080$.

*a*Kruskal-Wallis test.

*b*Mann-Whitney. Group differences present as Cohen's d (95% confidence interval) for the aviremic group vs. the control group for $CD3^{-}CD56^{+}$ (total NK), $CD3^{-}CD56^{dim}$, and $CD3^{+}CD56+$ in blood were 1.20 (0.06; 2.34), 1.23 (0.08; 2.37), and 1.95 (1.02; 2.89), respectively.